Dipron: An Eco-Friendly Corrosion Inhibitor for Iron in HCl Media in Both Micro and Nano Scale Particle Size - Comparative Study

Enas Mohamed Attia

Chemistry Department, Faculty of Science (Girls), AL-Azhar University, Nasr City, Cairo, Egypt
enasmattia@yahoo.com

Abstract

This study was performed in order to investigate the ability of using sulfa drug (Dipron) with heterogeneous particle size in both micro and nano scale forms as eco-friendly corrosion inhibitor for iron (Fe) in hydrochloric acid solutions, in addition to decide which form would be more effective to inhibit Fe corrosion. The particle size analysis for micro- and nano- scale Dipron was determined using BT-2001(Liquid) laser particle size analyzer and dynamic light scattering (DLS) respectively. Open circuit potential measurements, potentiodynamic and potentiostatic polarization techniques were performed at temperature range 20-60°C. The outcomes show that inhibition takes place by adsorption of the Dipron on Fe surface without altering the mechanism of corrosion process. The adsorption of Dipron on Fe surface is consistent with Langmuir's adsorption isotherm. Physical adsorption mechanism is proposed from the calculated activation energy and thermodynamic parameters for the two forms of Dipron. The negative values of free energy of adsorption (ΔG°_{ads}) indicate that adsorption of Dipron follows a spontaneous process. The obtained results indicate that nano- scale Dipron (NSD) has higher efficiency in corrosion inhibition than micro- scale Dipron (MSD). The inhibition efficiency increases with a corresponding increase in the inhibitor's concentration and decreases with rise of temperature.

Keywords: Corrosion, Inhibition, Adsorption, Potentiodynamic, Potentiostatic, micro-scale, nano- scale.

Introduction

Fe has a significant impact on our day – to – day life, directly or indirectly. The main reason behind large scale usage of this metal is that it is not very expensive as compared to other metals, and is also abundantly available on the surface of the earth. This metal which is the most commonly used corrodes in many media especially acidic one. The application of acid corrosion inhibitors in the industry is widely used to

prevent or minimize material loss during contact with acid [1]. Most of organic compounds which are largely used as corrosion inhibitors are toxic in nature. This revealed the need of environmentally friendly inhibitors. Recently, there is a growing interest on the development of drugs as inhibitors for metallic corrosion due to their non-toxic nature [2]. The choice of drugs used as corrosion inhibitors is based on the following facts: (a) the molecules have oxygen, nitrogen and sulphur as active centers, (b) they are healthy i.e. not hazardous and environmentally friendly and (c) they can be easily produced and purified [3]. Sulphonamides are drugs extensively used for the treatment of infections caused by gram-positive microorganisms, some fungi, and certain protozoa. Other therapeutic uses of sulfonamides are as diuretic and hypoglycemic agents. Dipron (one of the simplest sulphonamides) has numbers of functional adsorption centers (e.g. $-NH_2$ group, $-SO_2-NH-$ group and aromatic ring). It is strongly basic hence it can be readily soluble in the acid medium [4].

In view of the above, the aims of the present work are: (1) to make a comparative study on the inhibition of Fe corrosion in HCl solution by Dipron in both micro and nano scale forms using electrochemical methods. (2) to study the effect of temperature and concentration on the inhibitive properties of the drug in its two particle size scales. (3) to study the adsorption characteristics of the drug in its two scales by fitting the adsorption data into different adsorption models.

Experimental

Specimen's preparation

The specimen of Fe (99.99% purity, Alfa Ventron) with 1.643 cm^2 exposed area was made of massive cylindrical rod mounted into glass tube by epoxy resin. A copper wire was employed for an electrical contact. Before each experiment, the Fe surface was polished mechanically using emery papers of Grade Nos. 220, 400, 600, 800 and 1200, until its surface became smooth and mirror-like bright, then it was cleaned by washing thoroughly with distilled water and finally degreased with acetone.

Solutions and inhibitor

The aggressive solution was prepared by dilution of AR grade 37% HCl in bi-distilled water. The acid concentrations (0.05, 0.10, 0.25, 0.50, 0.75, 1.00 and 2.00 M) were prepared at 25°C.

The sulfa drug (Dipron), 4-(Aminosulfonyl)aniline, is of AR grade purchased from Nile Company for Pharmaceuticals and Chemical Industries and used as inhibitor without further purification. Its molecular weight is 172.2 g/mol with melting point and density 165 °C and 1.08 g/cm³, respectively. The chemical structure of Dipron is represented in Figure 1. The particle size of the purchased Dipron was determined using a high performance BT-2001(Liquid) laser particle size analyzer. Figure 2 represents the relation between diffraction and accumulation of Dipron molecules with its size.

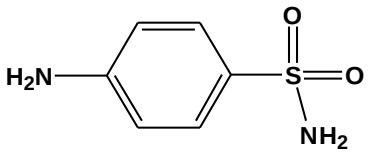

Figure 1: Chemical structure of Dipron: (4-(Aminosulfonyl)aniline)

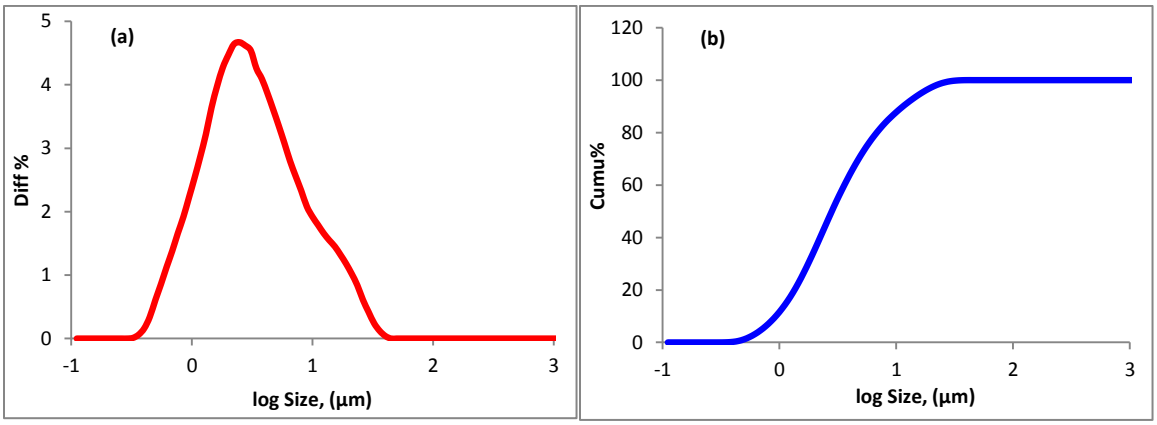

Figure 2: Relation between particle size with (a) diffraction and (b) accumulation of molecules.

The particle size analysis illustrate that the different percentages of particles with its different micro size are as follows: D3: 0.607 µm, D6: 0.754 µm, D10: 0.931 µm, D16: 1.182 µm, D25: 1.550 µm, D50: 2.811 µm, D75: 5.607 µm, D84: 8.160 µm, D90: 11.40 µm, D97: 19.55 µm and D98: 21.87 µm with medium index =1.00. On the other hand the percent of each present specified size in the system medium is illustrated in Table 1. Figure 2 and Table 1 illustrate the heterogeneity of the system

which all falls in the micro scale level. Thus purchased micro scale Dipron can be referred as MSD.

Table 1: Relation between particle size and its percentage in the medium

Size(μm)	0.323	0.548	0.929	1.576	2.674	4.537	7.698	13.060	22.160	37.670
Percent	0.00	1.94	9.94	25.62	47.88	68.38	82.74	92.06	98.10	100.00

The nano scale Dipron (NSD) was prepared by grinding MSD using ball mill at 200 rpm for 10 hours. The particle size of NSD was determined using dynamic light scattering (DLS). As can be seen from Figure (3), in number distribution technique, there is only one peak of 100% particle sizes equal to 159.4 nm. The polydispersity index value (PDI = 0.364) reflects the slightly mono-disperse in size and indicates that the sample has a relatively narrow size distribution with width equal to 89.68 nm.

Different concentrations of Dipron (0.19, 0.95, 1.90, 3.80, 9.50, 10.00 and 13.31 mM) were prepared at 25 °C by dissolving a calculated amount of the inhibitor in 0.5 M HCl.

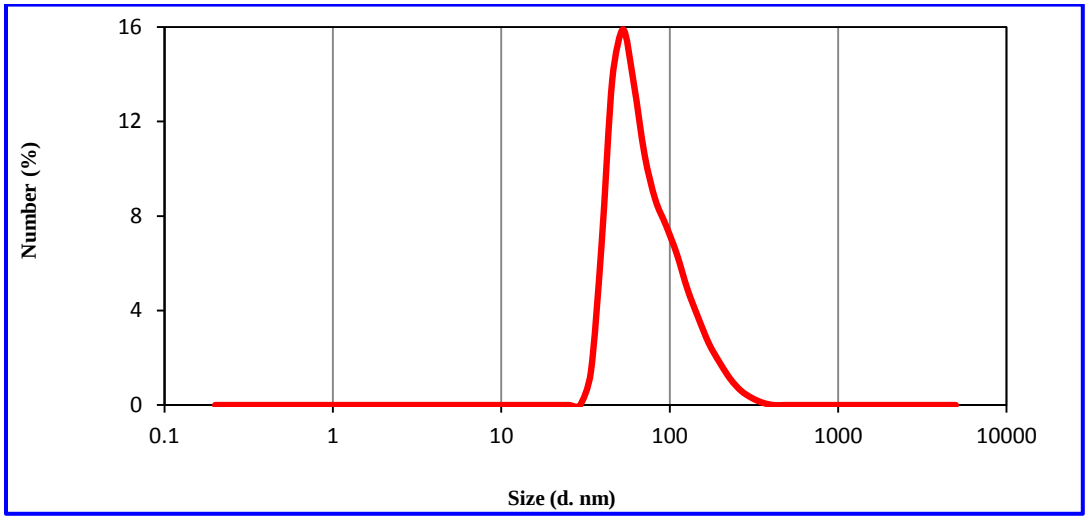

Figure 3: Size distributions of NSD by number.

Electrochemical techniques

Open circuit potential measurements

Open circuit potential (OCP) measurements were carried out in a double- walled glass cell filled with 25 ml of the test solution. The potentials were measured with the aid of digital multimeter (KEITHLEY, Model 175, USA) using saturated calomel electrode (SCE) as a reference electrode.

Potentiodynamic polarization

In potentiodynamic polarization technique, measurements were performed by changing the electrode potential from negative to positive direction at scan rate 3mV/s. The corrosion rate (C_R) in mpy was calculated using Eq.1 [5]:

$$C_R = 0.13 \times I_{corr} \times e/\rho \qquad (1)$$

where 0.13 is the metric and time conversion factor, I_{corr}, is the corrosion current density in μA/cm², e is the equivalent weight of metal in geq/mol and ρ, is the density in g/cm³. Values of I_{corr} and corrosion potential (E_{corr}) were determined from the extrapolation of linear Tafel segments of anodic and cathodic curves. The inhibition efficiency ($IE\%$) was evaluated from the measured I_{corr} values using Eq.2:

$$IE\% = \left[1 - \frac{I_{corr}}{I^{\circ}_{corr}}\right] \times 100 \qquad (2)$$

where I°_{corr} and I_{corr} are the corrosion current densities in absence and presence of inhibitor, respectively.

Potentiostatic polarization

In potentiostatic polarization, the experiments were undertaken by applying a constant voltage values (−150, −100, +10, +50, +100 and +200 mV(SCE)) to the working Fe electrode in 0.5 M HCl in absence and presence of Dipron in each of MSD and NSD forms and the corresponding current densities were recorded as a function of time.

The quantity of electricity (Q) passed through the metal surface was calculated from the relation $Q = It$, where I is the current density recoded corresponding to the applied voltage at time t. The surface charging capacity (C) is calculated from Eq. 3:

$$C = Q/V \qquad (3)$$

where V is the constant voltage applied across the metal surface. The reciprocal capacitance (C^{-1}) was in proportion to the thickness of the oxide film (d) according to Eq. 4 [6]:

$$d = \varepsilon\varepsilon^{\circ}AC^{-1} \qquad (4)$$

where A is the electrode surface area, ε is the dielectric constant of oxide and $\varepsilon^{\circ}$is the permittivity of free space $(8.845 \times 10^{-14}\ F/cm)$. Potentiodynamic and potentiostatic polarization measurements were generated using a Wenking Electronic Potentioscan (Mode l73). The indicated results are the mean of four experiments.

Results and Discussion

Open circuit potential measurements

Effect of different concentrations of Dipron on OCP of Fe electrode

Figure 4 illustrates the OCP of Fe immersed in 0.5 M HCl in absence and presence of different concentrations (0.19 –13.31 mM) of Dipron. The electrode potential shifts to more passive values in presence of Dipron in MSD and NSD forms compared with that of free HCl solution, indicating the inhibiting action of Dipron in its two forms. Considering the lowest (0.19 mM) and the highest (13.31mM) Dipron concentrations, the steady state potential (E_{ss}) is ranging from –353 to –337 mV(SCE) in presence of MSD and from –353 to –308 mV(SCE) in presence of NSD after 120 minute of immersion (E_{ss} of Fe in free 0.5 M HCl = –360 mV(SCE)). This means that at the studied concentrations, NSD shifts the electrode potentials to positive values more than MSD, indicating better effect on corrosion inhibition process in 0.5 M HCl. These results indicate that in OCP measurements, Dipron in both MSD and NSD forms stimulate the corrosion inhibition process in 0.5 M HCl and the effect of NSD is more pronounced than MSD. On the other hand, 10 mM Dipron concentration represents an odd behavior where its E_{ss} values are –290 and –302 mV(SCE) for MSD and NSD respectively. These values exceed that corresponding to the highest Dipron concentration (13.31 mM). Thus, 10 mM represents an optimum concentration for corrosion inhibition process in OCP measurements.

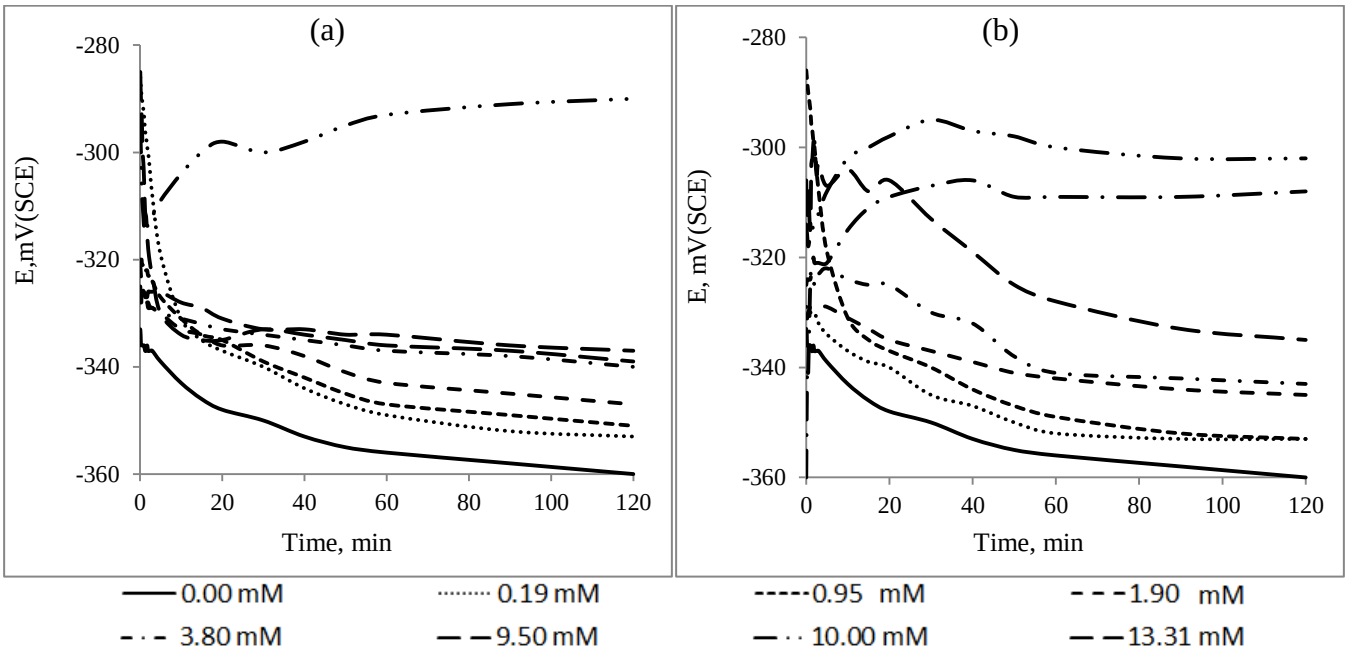

Figure 4: Effect of Dipron concentrations on OCP of Fe in 0.5 M HCl: (a) MSD, (b) NSD.

Effect of different concentrations of HCl in absence and presence of 10 mM Dipron on Fe electrode

The potentials of Fe electrode immersed in different concentrations (0.05–2.00 M) of HCl in absence and presence of 10 mM Dipron were measured as a function of immersion time as shown in Figure 5. The potentials of Fe electrode in free HCl (Fig. 5(a)) tends towards more negative potential represent the breakdown of the pre-immersion air formed oxide film present on the surface according to Eq.5 [7]:

$$Fe_2O_3 + 6HCl \rightarrow 2FeCl_3 + 3H_2O \qquad (5)$$

The general shift, to noble direction, points to oxidation of Fe_3O_4 to Fe_2O_3 according to Eq.6 [8].

$$4Fe_3O_4 + O_2 \rightarrow 6Fe_2O_3 \qquad (6)$$

Figure 5(b and c) indicates that addition of 10 mM Dipron in MSD and NSD forms to the medium produces a slight positive shift in the open circuit potential due to the retardation of the anodic reaction.

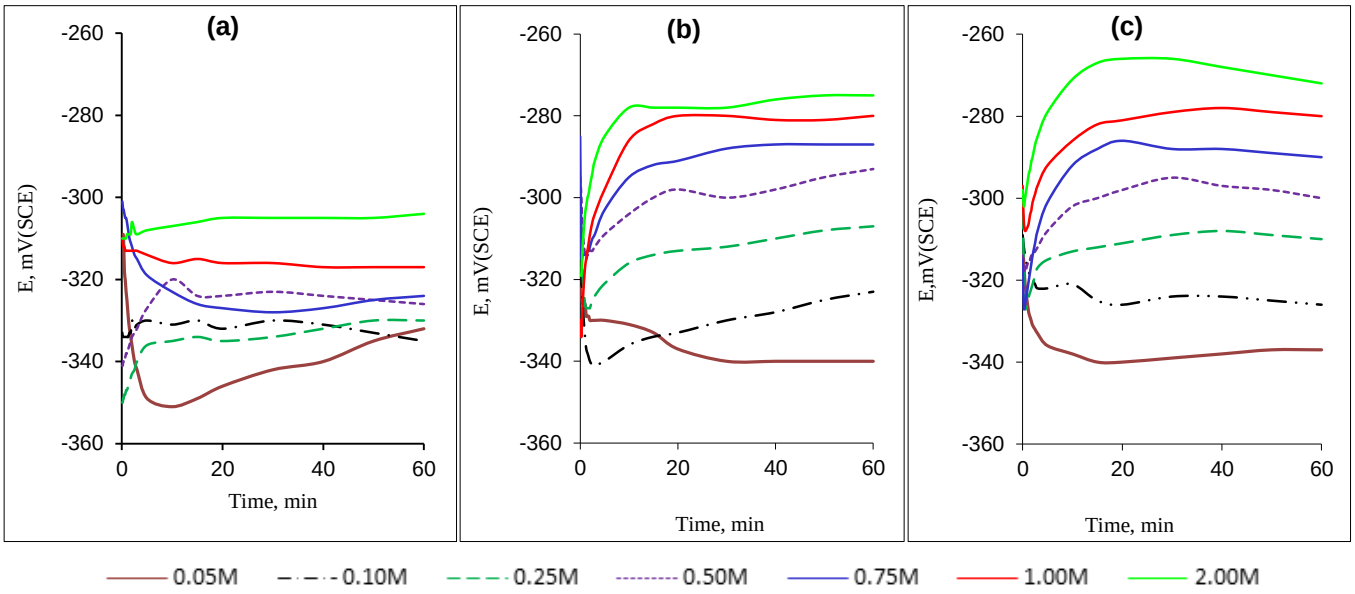

Figure 5: Potential – time curves of Fe in different concentrations of HCl in absence and presence of 10 mM Dipron: (a) Free HCl (b) MSD (c) NSD.

The variation of E_{ss} with the logarithm of the molar concentration, C, of the acid solutions, is represented in Figure 6. The results reveal that E_{ss} varies linearly with $\log C$ according to Eq. 7:

$$E_{ss} = \alpha + b \log C \qquad (7)$$

where, α represents the steady state potential in solution of 1 M concentration, and b is the slope of the straight line. The constants α and b are depending on the composition of solution. Values of α and b for Fe in free HCl are equal to −0.316 V(SCE) and 20 mV per decade concentration respectively. Addition of 10 mM Dipron in MSD and NSD forms shifts the steady state potentials positively with extrapolated values of α are −0.284 and −0.283 V(SCE) and values of b are 41 and 38 mV per decade concentration, respectively. These values indicate that 10 mM Dipron in MSD and NSD forms have similar inhibiting effect on open circuit potential of Fe in different concentrations of HCl solutions with preferential action of NSD form.

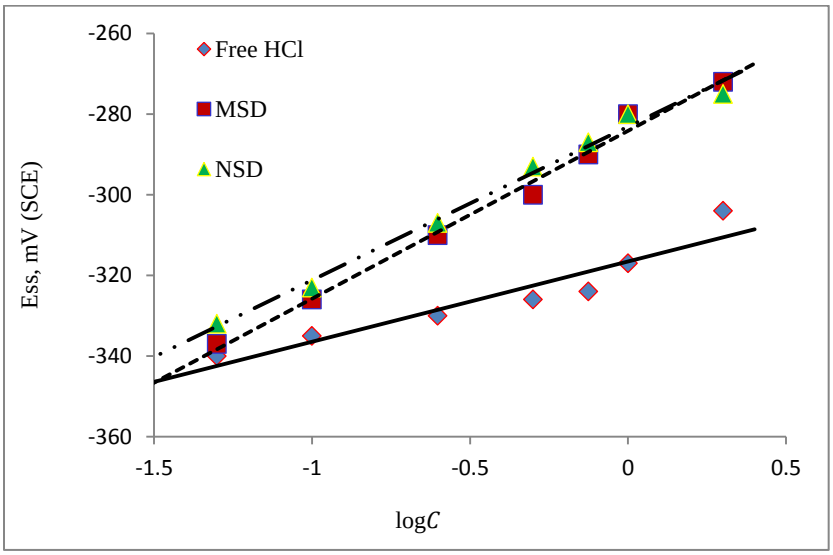

Figure 6: E_{ss} vs. $\log C$ for Fe in different concentrations of HCl solutions in absence and presence of 10 mM Dipron in MSD and NSD forms.

Potentiodynamic polarization measurements

Effect of HCl concentrations on corrosion behavior of Fe electrode

Polarization plots of Fe in different concentrations of HCl (0.05 – 2.00 M) at 25°C are shown in Figure 7. The respective potentiodynamic parameters including corrosion potential (E_{corr}), corrosion current density (I_{corr}), corrosion rate (C_R), anodic (b_a) and cathodic (b_c) Tafel slopes are listed in Table 2.

The analysis of the data in Table 2 revealed that I_{corr} and C_R increased with increasing acid concentration. This indicates that the aggressive Cl^- ions participate in the dissolution process. The Fe metal was oxidized at the anode where corrosion occurs according to Eq. 8:

$$Fe = Fe^{+2} + 2e^- \qquad (8)$$

Simultaneously, reduction occurs at cathodic sites according to Eq. 9:

$$2H^+ + 2e^- = H_2 \qquad (9)$$

Chloride ions typically migrate into Fe from the environment and, upon reaching embedded Fe and exceeding a certain critical concentration, destroys the passivating oxide layer on Fe forming complexes with ferrous ion. This led to formation of expansive corrosion products. Some of these products are soluble and assist transport

of corrosion products away from sites where they might otherwise give physical protection [9]. This corrosion process can be suppressed by using an appropriate dose of inhibitor, which reacts with and complex ferrous ions, or adsorbs on its surface thus interrupting the corrosion process.

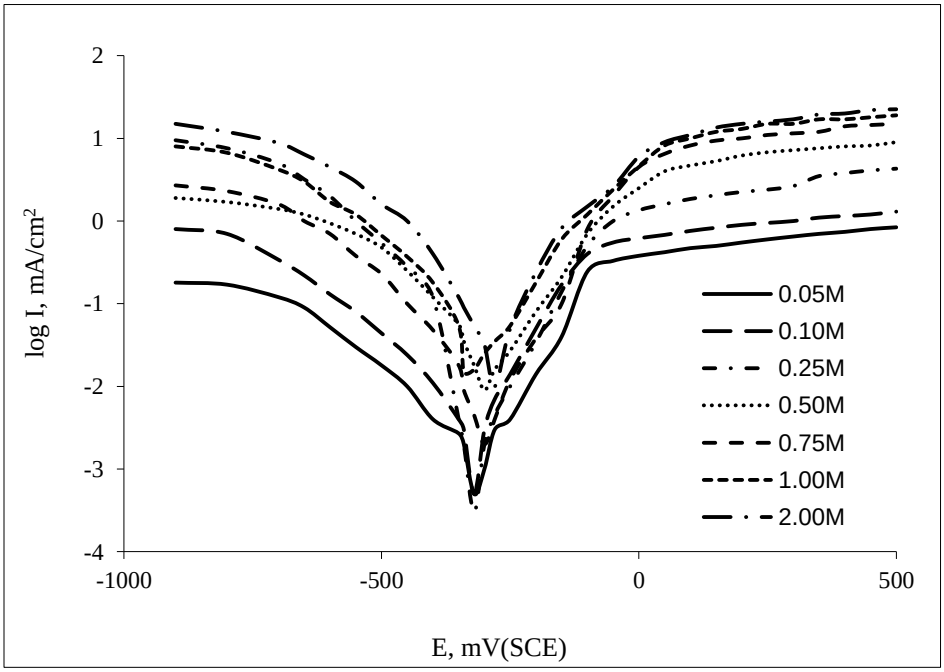

Figure 7: Potentiodynamic polarization plots of Fe in different concentrations of free HCl solutions.

Table 2: Potentiodynamic parameters of Fe in different concentrations of free HCl

C_{HCl} M	E_{corr} mV(SCE)	I_{corr} μA/cm²	C_R mpy	b_a mV/dec	$-b_c$ mV/dec
0.05	-320	100	46	100	200
0.10	-320	355	164	214	167
0.25	-320	950	439	94	36
0.50	-300	970	448	111	143
0.75	-300	1400	647	91	143
1.00	-340	1995	921	100	200
2.00	-280	2512	1160	91	100

Effect of HCl concentrations on the inhibition efficiency of 10 mM Dipron using Fe electrode

The effect of changing HCl concentrations on the inhibition efficiency of 10 mM Dipron was investigated in Figure 8 and the corresponding potentiodynamic parameters are represented in Table 3. It can be seen that, with increasing acid concentration and in the presence of 10 mM Dipron, the anodic and cathodic Tafel slopes changed greatly from that of free acid solutions (Table 2). This shows that addition of 10 mM Dipron to HCl solutions reduces the anodic dissolution of Fe and delays the hydrogen evolution reaction. The presence of Dipron in MSD and NSD forms lowered both of I_{corr} and C_R of Fe electrode compared with obtained values of free HCl. Moreover NSD achieved lower I_{corr} and C_R values than MSD. Also, increasing acid concentration resulted in decreasing IE% in the presence of the two forms of Dipron. Thus, at high acid concentration, the adsorbed inhibitor molecules could be expected to be desorbed by the retardation action of Cl^- ions [10].

The results illustrated that adsorbed NSD was stronger than MSD form. The inhibition efficiency in presence of 10 mM NSD reached its maximum value, 98.22 %, at 0.05 M HCl, and it is higher than that of MSD which reached to 91.60 % at the same concentration. This may be due to the presence of smaller nano particles of inhibitor in case of NSD form. However, as the size of a particle decreases, its surface area increases and also allows a greater proportion of its atoms or molecules to be displayed on the surface rather than the bigger molecules [11].

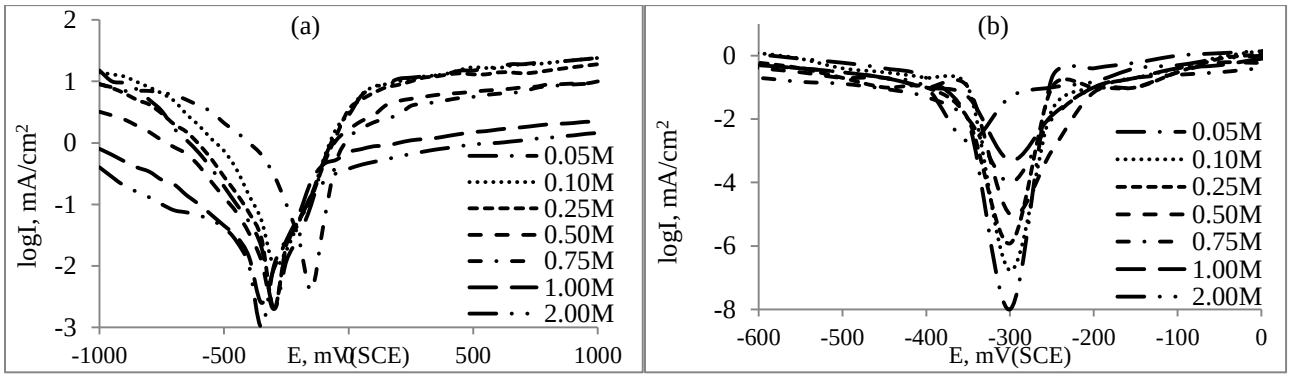

Figure 8: Potentiodynamic polarization plots of Fe in presence of 10 mM Dipron soluble in different concentrations of HCl solutions: (a) MSD, (b) NSD

Table 3: Potentiodynamic parameters of Fe in different concentrations of HCl solutions in presence of 10 mM Dipron in MSD and NSD forms

Medium	C_{HCl} M	E_{corr} mV(SCE)	I_{corr} $\mu A/cm^2$	C_R mpy	b_a mV/dec	$-b_c$ mV/dec	IE%
10 mM MSD	0.05	−350	84	4	167	154	91.60
	0.10	−350	40	18	222	318	88.72
	0.25	−150	120	55	250	214	87.37
	0.50	−300	138	64	222	400	85.77
	0.75	−300	200	92	222	375	85.71
	1.00	−300	300	138	167	250	84.96
	2.00	−300	400	185	200	250	84.07
10 mM NSD	0.05	−350	2	0.82	75	50	98.22
	0.10	−300	8	3.69	50	50	97.74
	0.25	−300	30	13.8	40	31	96.84
	0.50	−300	40	18.4	182	29	95.88
	0.75	−300	68	31.4	20	31	95.14
	1.00	−300	100	46.1	21	17	94.98
	2.00	−300	250	115.4	11	18	90.05

The natural logarithms of C_R of Fe in absence and presence of 10 mM MSD and NSD versus the molar concentration of HCl (C_{HCl}) illustrate a straight line broken at approximately 0.25 M HCl for all solutions. The following rate equation was set up to describe the straight line relationship [12].

$$\ln C_R = \ln K + \beta C_{HCl} \qquad (10)$$

where K is the specific corrosion reaction rate constant and β is a constant for the reaction. Equation 10 is shown graphically in Figure 9 and the calculated kinetic parameters are listed in Table 4. It is clear from Figure 9 and Table 4 that in the presence of MSD and NSD, the magnitude of C_R is suppressed as its tendency to increase with increasing acid concentrations. This may be due to suppression of Fe chloride by the adsorption of Dipron molecules [10]. The decrease of slope of the second part of broken lines may be arise from the formation of a tightly adsorbed, more protective Fe chloride compound on the metal at higher acid concentrations (>

0.25 M) [12]. On the other hand, the presence of 10 mM NSD soluble in different concentrations of HCl considerably decrease the magnitude of C_R compared with that of MSD. β_1 and K_1 in Table 4 represent the defined constants of equation 10 at acid concentrations of 0.05, 0.10 and 0.25 M HCl. While β_2 and K_2 represent the same constants at acid concentrations of 0.50, 0.75, 1.00 and 2.00 M HCl. Data in Table 4 illustrates that, the constants β_1 and β_2 for inhibited solutions are higher than that for free HCl solutions. The rate constants of corrosion reaction, K_1 and K_2, decrease in the following order: Free HCl > MSD > NSD. This indicates the inhibiting action of Dipron and the better action of NSD form.

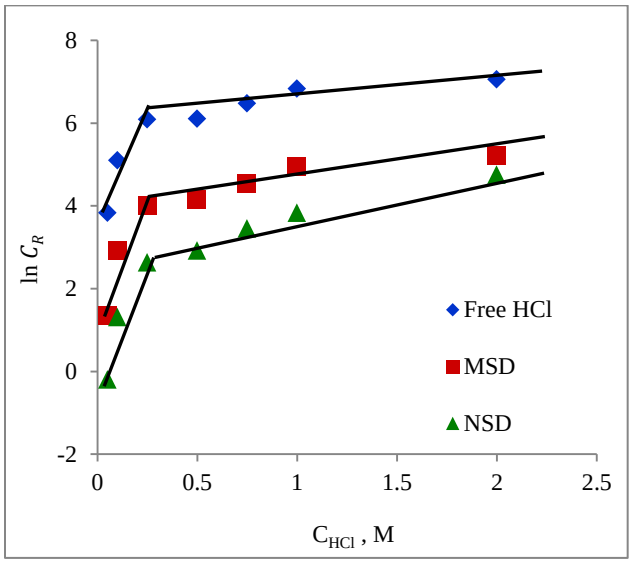

Figure 9: Variation of lnC_R of Fe with different concentrations of HCl in absence and presence of 10 mM Dipron in MSD and NSD forms at 25 °C.

Table 4: kinetic parameters for the corrosion of Fe in HCl solutions in absence and presence of 10 mM Dipron in MSD and NSD forms

Medium	β_1	β_2	k_1	k_2
	mpy M		mpy	
Free HCl	25.33	0.59	1.30E-2	394
MSD	31.21	0.70	8.14E-4	51
NSD	30.06	1.21	1.83E-4	11

Effect of different concentrations of Dipron on corrosion behavior of Fe electrode

The effect of different concentrations of MSD and NSD on the potentiodynamic polarization of Fe is represented in Figure 10. From the figure it can be observed that the addition of different concentrations of NSD to 0.5 M HCl shifts the anodic and cathodic branches of polarization curves of free acid solution towards lower current densities than MSD does. The potentiodynamic parameters of Dipron in the two forms are illustrated in Table 5. The values of I_{corr} and C_R decrease with increasing Dipron concentration. This decrement indicates that the addition of Dipron molecules inhibits the corrosion process by decreasing the surface area for corrosion. This demonstrates that Dipron acts as inhibitor by adsorption onto Fe surface, and the inhibition degree depends on the nature of inhibitor and its concentration. Both b_a and b_c values changes noticeably in presence of the two forms of inhibitor than that observed in free acid solution. The inhibition efficiencies increase with increasing Dipron concentration. The highest IE% of 97.9 occurred at 13.31 mM NSD compared with 89.7 for MSD. This is most likely due to the adsorption and formation of a good protective film by Dipron in MSD and NSD forms. The formation of a protective film is a result of the interaction of Dipron molecules with atoms of the Fe surface. The smaller NSD particles present in HCl solution have high surface area that provides high reaction activities leading to an increase in the formation of a protective film [13].

Values of corrosion potential are not affected by addition of any concentration of MSD indicating that this form could act as pickling inhibitor which in spite of leaving the corrosion potential virtually unaffected, cause a significant decrease in the corrosion rate [10]. The same behavior was recorded for NSD at concentrations 3.80, 9.50, 10.00 and 13.31 mM. On the other hand, a positive displacement of the E_{corr} values exhibited by 0.19 mM NSD was 200 mV(SCE) and by 0.95 and 1.90 mM was 100 mV(SCE). This means that, at these concentrations, the dissolution of the anode can be controlled and the hydrogen evolution controlling process is reduced. An inhibitor can be classified as anodic or cathodic type when the change in E_{corr} value is higher than 85 mV in relation to that measured for the free solution [14]. Hence, it can be concluded that NSD form could act as pickling inhibitor at high concentrations and behaves as mixed type but predominantly anodic inhibitor at low concentrations.

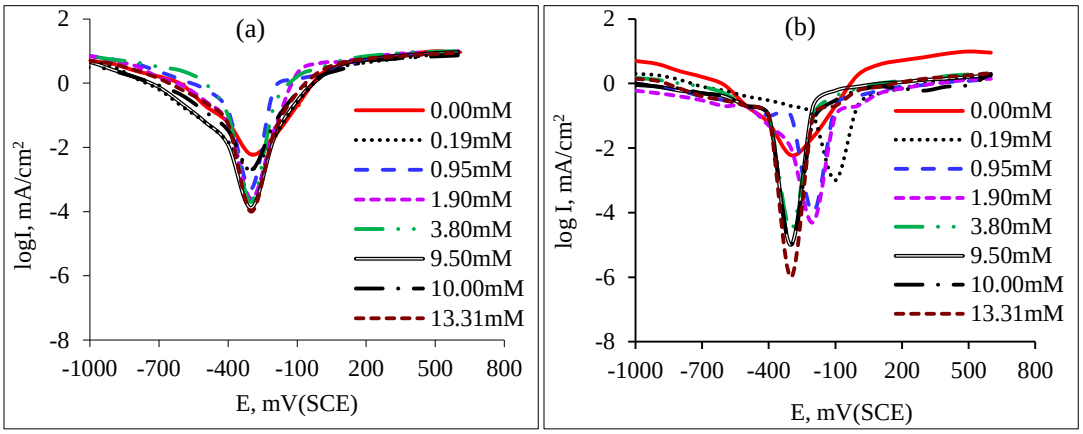

Figure 10: Potentiodynamic polarization plots of Fe electrode in different concentrations of Dipron in its two form: (a) MSD, (b) NSD.

Table 5: Potentiodynamic parameters of Fe in 0.5M HCl in absence and presence of different concentrations of MSD and NSD at 25 °C

Medium	C_{inh} mM	E_{corr} mV(SCE)	I_{corr} μA/cm²	C_R mpy	b_a mV/dec	$-b_c$ mV/dec	IE%
Free HCl	0.00	-300	970	448	111	143	-
MSD	0.19	-300	316	146	185	200	67.4
	0.95	-300	200	92	100	160	79.4
	1.90	-300	180	83	100	200	81.4
	3.80	-300	160	74	100	100	83.5
	9.50	-300	145	67	133	171	85.0
	10.00	-300	140	64	222	400	85.6
	13.31	-300	100	46	142	250	89.7
NSD	0.19	-100	100	46	360	560	89.7
	0.95	-200	60	28	228	133	93.8
	1.90	-200	49	22	333	160	94.9
	3.80	-300	45	21	314	280	95.3
	9.50	-300	42	19	300	366	95.7
	10.00	-300	40	18	182	29	95.9
	13.31	-300	20	9	267	533	97.9

Adsorption isotherms

Freundlich isotherm

The Freundlich isotherm model was chosen to explain the adsorption of Dipron on the iron surface with uniform energy according to Eq. 11 [10, 15]:

$$\theta = K_{ads} C_{inh}^{\frac{1}{n}} \qquad (11)$$

The linearized form is given in Eq. 12:

$$\log\theta = \log K_{ads} + \frac{1}{n}\log C_{inh} \qquad (12)$$

where, K_{ads} (the equilibrium constant) and $\frac{1}{n}$ are indicators of the adsorption capacity and adsorption intensity respectively. C_{inh} is the inhibitor concentration (mM) and θ is the surface coverage degree. Figure (11-a) represents the adsorption of MSD and NSD on Fe surface according to this model. The adsorption parameters are listed in Table 6 and compared with that of Langmuir model.

It has been stated that the magnitude of $\frac{1}{n}$ gives an indication of the favorability and capacity of the adsorbent/adsorbate system. A value for $\frac{1}{n} < 1$ as in the present study indicates a normal Freundlich isotherm in which a significant adsorption takes place at low concentration but the increase in the amount adsorbed with concentration becomes less significant at higher concentrations and vice versa, while $\frac{1}{n} > 1$ is indicative of cooperative adsorption [10, 16]. Also, the higher K_{ads} value for NSD indicates the greater the adsorption capacity. K_{ads} is related to the free energy of adsorption, ΔG_{ads}° , by Eq. 13:

$$K_{ads} = (1/55.5)\exp -\left(\Delta G_{ads}^{\circ}/RT\right) \qquad (13)$$

where 55.5 is the molar concentration of water, R is the universal gas constant and T is the absolute temperature.

The obtained negative value of ΔG_{ads}° indicates that the adsorption process of Dipron in MSD and NSD forms on the Fe surface is spontaneous.

Langmuir isotherm

A mathematical representation of the Langmuir model is illustrated in Eq. 14 [10, 17]:

$$C_{inh}/\theta = 1/K_{ads}\, B_s + C_{inh}/B_s \qquad (14)$$

where B_s, is the adsorbate binding capacity, that is, the maximum adsorption upon complete saturation of adsorbent surface.

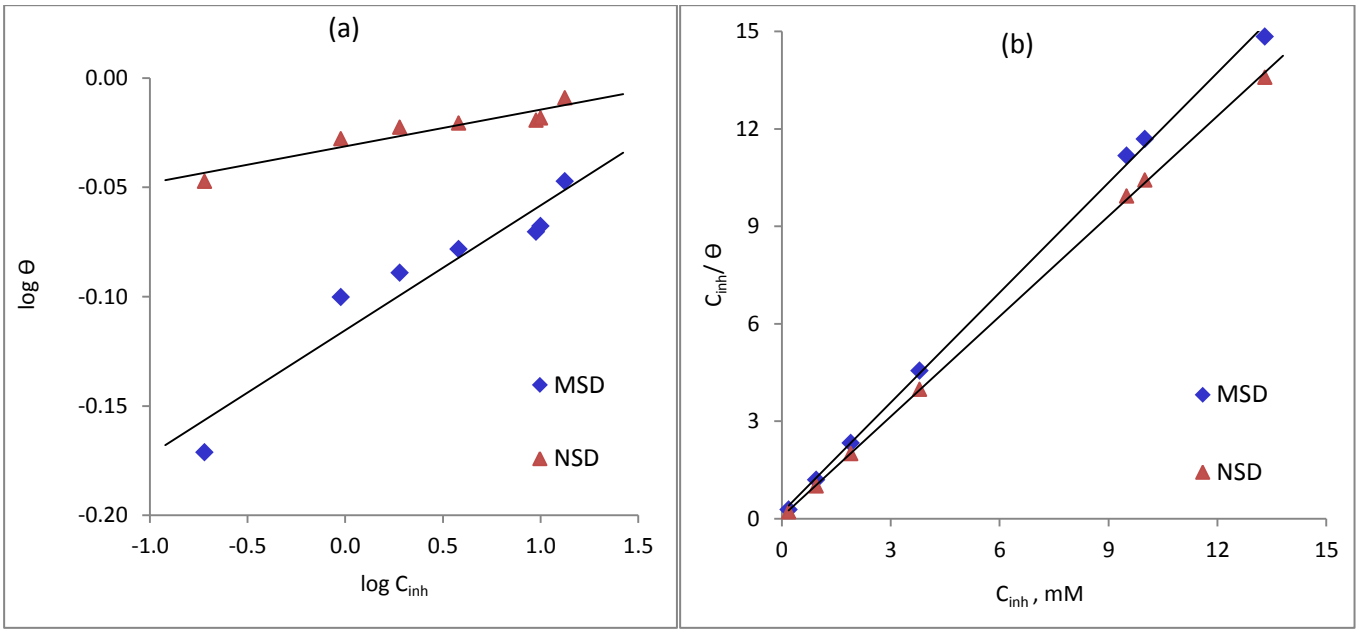

Figure 11: Adsorption isotherms of Dipron in MSD and NSD form on Fe surface: (a) Freundlich, (b) Langmuir.

Figure (11-b) and Table 6 show that for Langmiure adsorption isotherm, the linear correlation coefficients (R^2) and the slopes of the two forms of Dipron are almost very close to unity, which indicates that the adsorption of Dipron in the micro and nano scales follows Langmuir adsorption isotherm. This means that the solid surface contains a fixed number of adsorption sites and each site holds one adsorbed species [18]. The higher values of K_{ads} and B_s suggested higher capacity of the adsorption process and stability of the adsorbed layer on the Fe surface in the presence of NSD than that in presence of MSD. Values of ΔG°_{ads} between 0 and -20 kJ/mol, as in the present study, are consistent with spontaneous physical adsorption [19].

Table 6: Freundlich and Langmuir isotherms constants for adsorption of Dipron in MSD and NSD forms on Fe surface at 25 ℃

Isotherm	MSD	NSD
Freundlich isotherm		
R^2	0.913	0.890
K_{ads}, mol^{-1}	0.766	0.931
n	17.513	59.523
$1/n$	0.057	0.017
ΔG°_{ads}, kJ/mol	−9.293	−9.773
Langmuire isotherm		
R^2	0.998	0.999
slope	1.128	1.027
B_s	0.886	0.973
K_{ads}, mol^{-1}	4.660	16.860
ΔG°_{ads}, kJ/mol	−13.765	−16.949

Effect of temperature on the corrosion behavior of Fe in 0.5 M HCl in absence and presence of 10 mM Dipron

Temperature is an important parameter in the metal dissolution studies. The effect of temperature on the inhibition of metal corrosion reactions is very complex because different changes may occur on the metal surface such as rapid etching, desorption of inhibitor and the inhibitor may undergo decomposition [20].

In this study, the effect of changing the temperature from 20 to 60 ℃ on the corrosion behavior of Fe in free 0.5 M HCl and in presence of 10 mM of Dipron in both of MSD and NSD forms was studied. It was observed that variation of temperature has almost no effect on the general shape of the polarization curves as shown in Figure 12. Table 7 illustrates the effect of temperature on the corrosion potentials and corrosion rates of Fe in 0.5 M HCl in absence and presence of 10 mM Dipron in MSD and NSD forms and its corresponding inhibition efficiencies. By increasing the temperature, the corrosion rates increases and the free acid solution showed maximum corrosion rates than that in the presence of Dipron. This signified that the dissolution of the metal increased at higher temperatures. This is because the reactant molecules gain more

energy and are able to overcome the energy barrier more rapidly. An increase in temperature may also increase the solubility of the adsorbed films on the metals, thus increasing the susceptibility of the metal to corrosion [21]. The decrease in IE% with the increase in temperature might be attributed to the weakening of the physical adsorption process of inhibitor on the metal surface. For a physical adsorption mechanism, IE% of an inhibitor decreases with increasing temperature while for a chemical adsorption mechanism, values of inhibition efficiency increases with temperature [21].

It is noted from Table 7 that MSD has the best IE% value at 20 ℃ whereas the inhibition efficiency decreased at higher temperatures. On the other hand NSD keeps its tendency for inhibition efficiency constant even at higher temperatures owing to its greater activity which resulted from the presence of smaller nano particle size in the corrosive HCl solution.

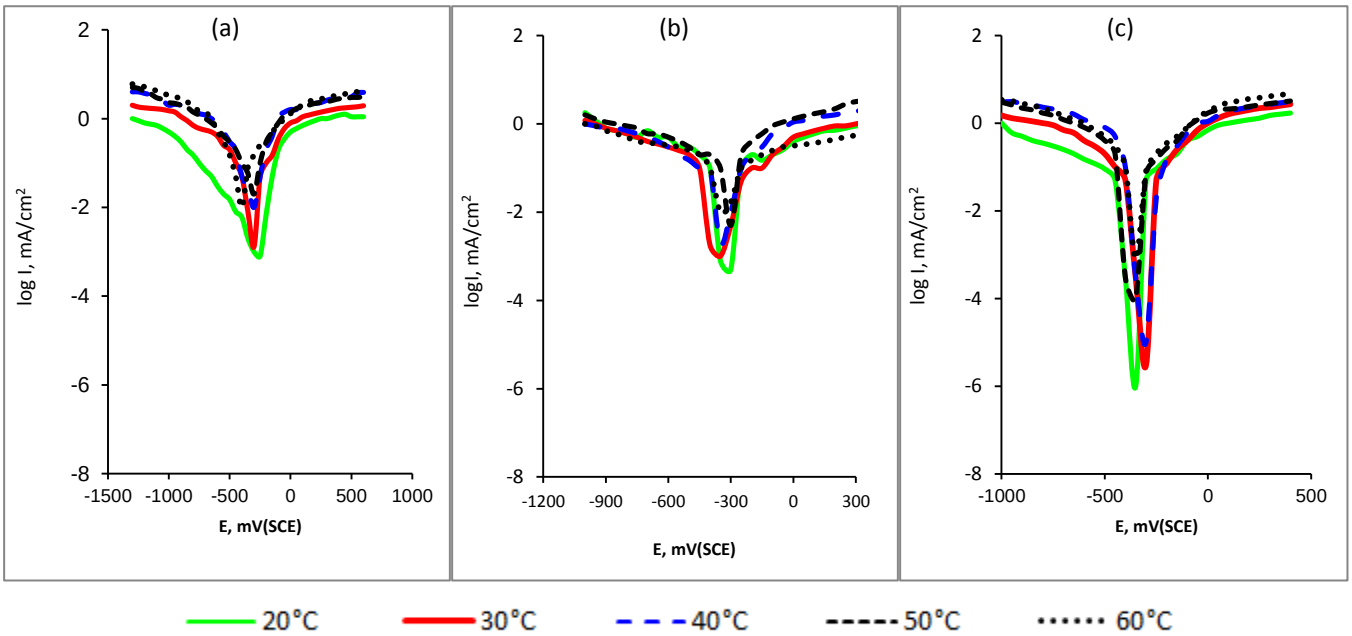

Figure 12: Effect of temperature on potentiodynamic polarization of Fe electrode in 0.5M HCl in absence and presence of 10 mM Dipron: (a) free HCl (b) MSD (c) NSD.

Table 7: Corrosion potential and corrosion rates of Fe electrode in 0.5M HCl in absence and presence of 10 mM of Dipron in MSD and NSD forms and the corresponding inhibition efficiencies at different temperatures

	Free HCl		MSD			NSD		
T ˚C	E_{corr} mV(SCE)	C_R mpy	E_{corr} mV(SCE)	C_R mpy	IE%	E_{corr} mV(SCE)	C_R mpy	IE%
20	−250	369	−300	23.1	93.75	−350	6.9	98.13
30	−300	453	−350	64.7	85.71	−300	18.9	95.82
40	−300	508	−350	73.9	85.45	−300	22.2	95.64
50	−300	647	−300	97.9	84.85	−350	28.6	95.57
60	−400	785	−350	161.6	79.41	−350	35.1	95.53

The dependence of corrosion rate, C_R, on temperature can be expressed by the Arrhenius equation [20]:

$$\log C_R = A - (E_a/2.303\,RT) \qquad (15)$$

where A is a constant representing the frequency factor, E_a is the apparent activation energy of the Fe dissolution reaction, R is the universal gas constant and T is the absolute temperature. The values of E_a can be calculated from the slopes of the straight line obtained by plotting $\log C_R$ vs $1/T$ as illustrated in Figure 13(a). The thermodynamic functions for dissolution of Fe in 0.5M HCl in absence and presence of 10 mM of Dipron in MSD and NSD forms were obtained by applying the Eyring transition-state equation (Eq. 16) [18, 20]:

$$\log C_R/T = \log(R/Nh) + (\Delta S^{\circ}/2.303R) - (\Delta H^{\circ}/2.303RT) \qquad (16)$$

where N is Avogadro's number, h is Planck's constant, ΔS° and ΔH° are the entropy and enthalpy of activation, respectively. A plot of $\log C_R/T$ vs. $1/T$ gave straight line with slope of [—$\Delta H^{\circ}/2.303R$] and an intercept of [$\log(R/Nh) + (\Delta S^{\circ}/2.303R)$] as illustrated in Figure 13 (b). The obtained values were tabulated in Table 8.

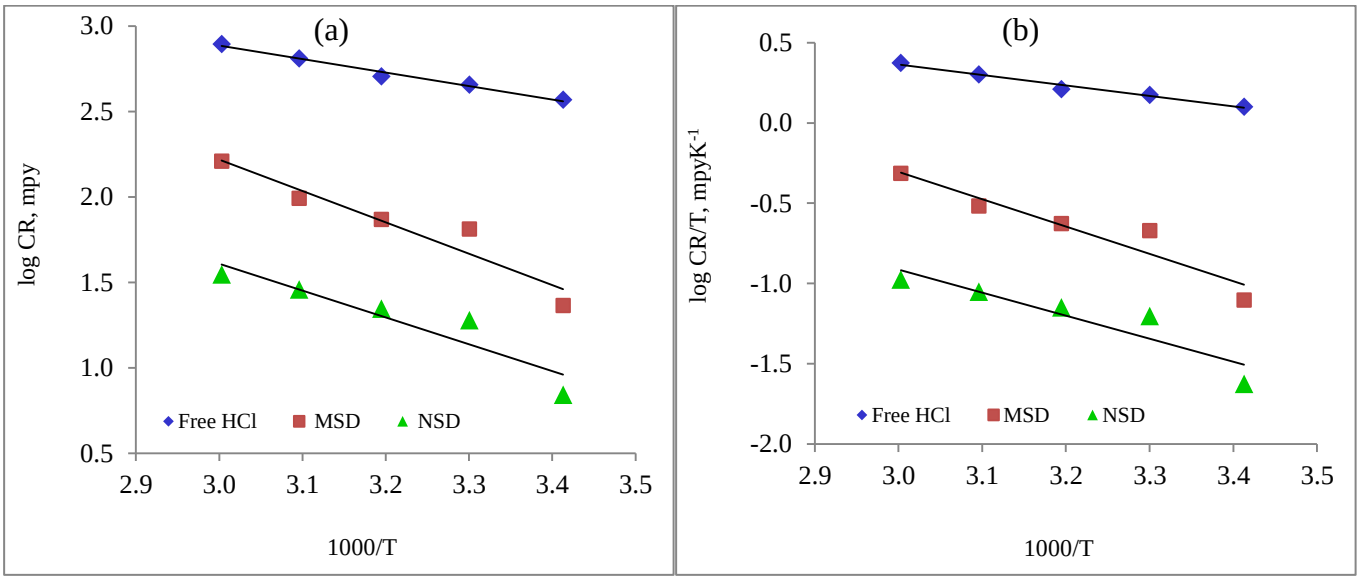

Figure 13: (a) Arrhenius plot, (b) Transition state plot.

Table 8: Activation parameters of Fe in 0.5M HCl in absence and presence of 10 mM Dipron

Medium	E_a kJ/mol	ΔH° kJ/mol	ΔS° J/mol K
Free HCl	15	12	-153
MSD	35	32	-106
NSD	30	27	-133

The increase in E_a and ΔH° in the presence of MSD and NSD forms implies that addition of Dipron to the acid solution increases the height of the energy barrier of the corrosion reaction and indicating that as the temperature is raised a decrease in protection efficiency is obtained [22]. It is noted from Table 8 that E_a for the corrosion process, in presence of Dipron, is greater than 20 kJ/mol and hence the entire process is controlled by surface reaction [23]. Based on the temperature effects, the relationships between the temperature dependence of IE% of an inhibitor and the E_a can be classified into three groups [24]:

(1) IE% decreases with the increase in temperature: E_a (inhibited solution) $>$ E_a (uninhibited solution);
(2) IE% increases with the increase in temperature: E_a (inhibited solution) $<$ E_a (uninhibited solution);
(3) IE% does not change with temperature: E_a (inhibited solution) $=$ E_a (uninhibited solution).

According to Tables 7 and 8, group (1) is the applied case in which the values of E_a suggests the physisorption mechanism. The positive signs of ΔH° reflect the endothermic nature of Fe dissolution process which suggests its difficult and slow dissolution in presence of Dipron in MSD and NSD forms [18]. Values of entropy of activation (ΔS°) illustrated less negativity for inhibited solutions than that for the uninhibited one. This implied that the activated complex represents an association rather than a disordering going from reactants to the activated complex [18]. This reflects the formation of an ordered stable layer of inhibitor on the Fe surface [25]. Thus, one can say the nature of inhibitor and the temperature of solution affect greatly the activation parameters of the corrosion process.

Potentiostatic polarization

Effect of applied potential

Figure 14(a, b and c) shows the variation of current density with time at different applied potentials (E_A) for Fe electrode in 0.5M HCl in absence and presence of 10 mM Dipron in MSD and NSD forms, respectively. The corresponding values of initial current density (i_i), stabilized current density (i_s), quantity of electricity (Q) and surface charging capacity (C) are summarized in Table 9. It is clear that, for each type of solution, as a general trend, the i_i, i_s and Q increases by increasing the applied potentials. Comparing the three types of solutions, values of i_i, i_s, Q and C for Fe electrode generally decreases in the following order:

Free HCl $>$ MSD $>$ NSD

This illustrates the effective action of Dipron in MSD and NSD forms on the corrosion inhibition of Fe in 0.5M HCl and ensured the better action of NSD form.

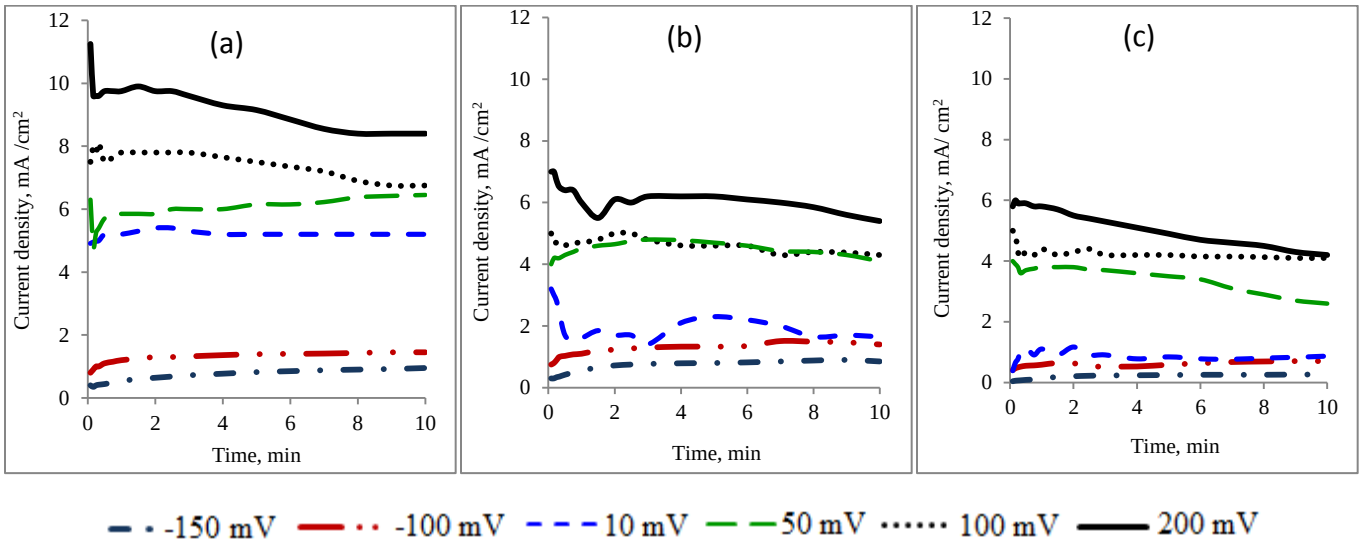

Figure 14: Potentiostatic polarization plots of Fe electrode at different applied potentials in 0.5M HCl in absence and presence of 10 mM Dipron: (a) free HCl (b) MSD (c) NSD.

These results are in good agreement with those obtained in OCP and potentiodynamic polarization measurements.

The highest Q values observed for free 0.5M HCl were due to the preferential adsorption of Cl^- ions on the oxide surface acting as a depolarizer for the main anodic process of oxygen discharge [26]. The results showed that the surface charging capacity reached its maximum value at 10 mV(SCE) in the three types of solutions.

Effect of inhibitor concentration

Figure 15 and Table 10 illustrate the effect of Dipron concentration at constant applied voltage of 10 mV(SCE) on the potentiostatic behavior of Fe in 0.5 M HCl at 25 ℃. It is clearly observed that the presence of different concentrations of Dipron in MSD and NSD forms was accompanied by a reduction in stabilized current density compared with that recorded for free acid solution. The current densities decreased with increasing inhibitor concentrations. This was an indicative of passivation of the electrode in the presence of the two forms of Dipron. The decrease in C values in the presence of inhibitor is attributed to a decrease in active sites because of the adsorbed Dipron in micro and nano scale particle size [27]. The values of film thickness (d) did not change regularly with the Dipron concentration. But in all cases, it is higher in the

Table 9: Potentiostatic parameters of Fe in 0.5M HCl in absence and presence of 10 mM Dipron in MSD and NSD forms at different applied potentials at 25 °C

Medium	E_A mV(SCE)	i_i mA/cm²	i_s mA/cm²	Q mC/cm²	C mF/cm²
Free HCl	-150	0.40	0.95	85	0.57
	-100	0.80	1.45	130	1.31
	10	4.91	5.20	1092	109.20
	50	6.30	6.45	290	5.81
	100	7.50	6.75	1012	10.12
	200	11.25	8.40	1008	5.04
MSD	-150	0.30	0.85	76	0.51
	-100	0.75	1.40	84	0.84
	10	3.20	1.65	198	19.80
	50	4.00	4.10	184	3.69
	100	5.00	4.30	645	6.45
	200	7.00	5.40	972	4.86
NSD	-150	0.04	0.26	24	0.16
	-100	0.41	0.71	42	0.42
	10	0.39	0.87	157	15.68
	50	4.00	2.60	156	3.12
	100	5.00	4.10	615	6.15
	200	5.80	4.20	630	3.15

presence of Dipron than that of free acid solution, and in most cases it is higher in the presence of NSD compared with MSD indicating its better protective properties. It is worthy to mention that 10 mM Dipron concentration show better protective properties than other concentrations and can be considered as an optimum concentration for this study. This result is in good agreement with that obtained in OCP measurements.

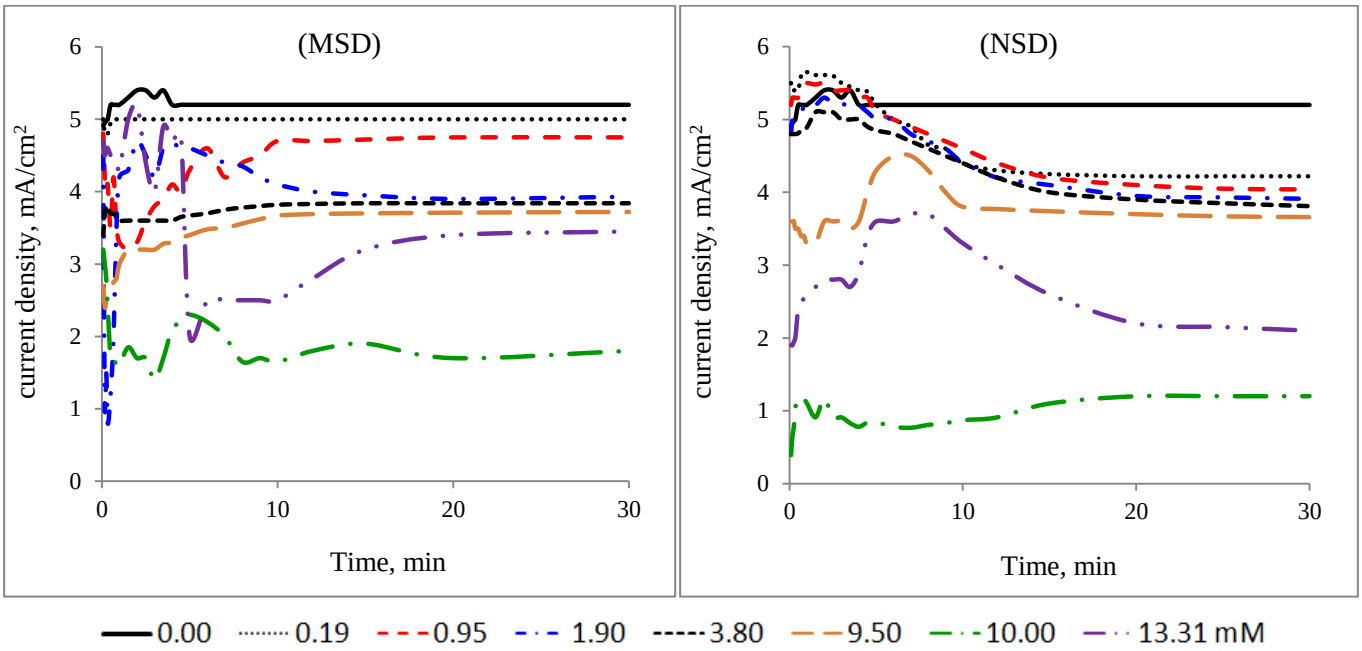

Figure 15: Potentiostatic polarization plots of Fe in 0.5 M HCl in absence and presence of different concentrations of Dipron at constant applied voltage of 10 mV(SCE).

Table 10: Potentiostatic parameters of Fe in 0.5 M HCl in absence and presence of different concentrations of Dipron at constant applied voltage of 10 mV(SCE) at 25°C

	MSD				NSD			
C_{inh} mM	i_i mA/cm²	i_s mA/cm²	C mF/cm²	d Å*10⁻⁶	i_i mA/cm²	i_s mA/cm²	C mF/cm²	d Å*10⁻⁶
0.00	4.91	5.20	109.20	1.89	4.91	5.20	109.20	1.89
0.19	5.00	5.00	60.00	3.45	5.50	4.22	25.32	8.17
0.95	4.80	4.75	57.00	3.63	5.20	4.04	24.24	8.54
1.90	4.50	3.93	82.53	2.51	4.80	3.91	19.54	10.59
3.80	3.40	3.84	80.64	2.56	4.80	3.81	45.72	4.53
9.50	2.70	3.72	78.12	2.65	3.60	3.66	76.86	2.69
10.00	3.20	1.80	86.40	2.40	0.39	1.20	21.60	9.58
13.31	4.70	3.45	103.50	2.00	1.90	2.10	37.80	5.47

Effect of temperature

Figure 16 represents the temperature effect on corrosion behavior of Fe electrode immersed in 0.5 M HCl in absence and presence of 10 mM Dipron in MSD and NSD forms at constant applied voltage of 10 mV(SCE). The potentiostatic parameters are tabulated in Table 11. It is clear that, for the three types of solutions, i_i, i_s, Q and C, all generally increase with increasing temperature obeying the following order: Free HCl $>$ MSD $>$ NSD. This can be attributed to an appreciable decrease in the adsorption of Dipron on the Fe surface with increase in temperature and a corresponding increase in corrosion rates expected due to the fact that greater area of metal is exposed to acid environment. The reciprocal capacitances which represent the film stability are always having higher values for acid solutions containing NSD than that containing MSD at all temperatures. From Figure 16 and Table 11 it can be concluded that the presence of Dipron in its two forms inhibit the corrosion of Fe in 0.5 M HCl. Also, the presence of NSD in 0.5 M HCl solution resists the increasing Fe corrosion accompanied by increasing temperature more effectively than MSD does.

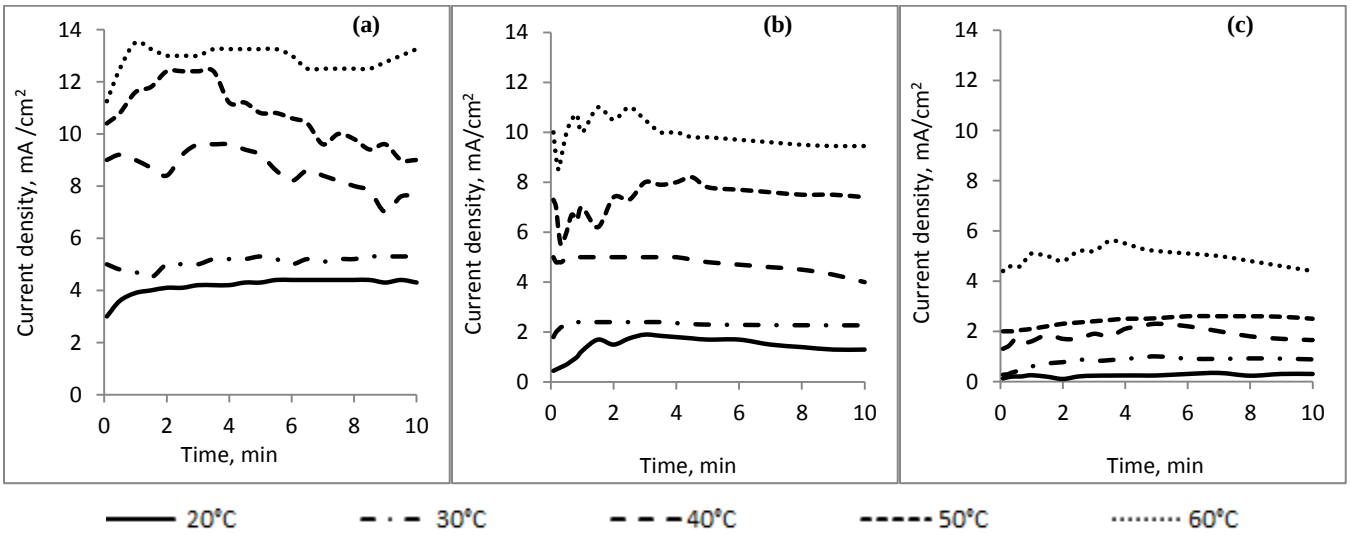

Figure 16: Effect of temperature on Fe electrode at constant applied voltage of 10 mV(SCE) in 0.5M HCl in absence and presence of 10 mM Dipron: (a) free HCl (b) MSD (c) NSD.

Table 11: Potentiostatic parameters of Fe electrode in 0.5 M HCl in absence and presence of 10 mM Dipron in MSD and NSD forms at constant applied voltage of 10 mV(SCE) at different temperatures

Medium	Temp. °C	i_i mA/cm²	i_s mA/cm²	Q mC/cm²	C mF/cm2	C^{-1} cm²/mF
Free HCl	20	3.00	4.30	258	25.80	3.88E-02
	30	5.00	5.30	636	63.60	1.57E-02
	40	9.00	7.60	912	91.20	1.10E-02
	50	10.40	9.00	270	27.00	3.70E-02
	60	11.25	13.25	795	79.50	1.26E-02
MSD	20	0.45	1.30	156.00	15.60	6.40E-02
	30	1.80	2.27	204.30	20.43	4.89E-02
	40	5.00	4.00	480.00	48.00	2.08E-02
	50	7.30	7.40	1332.00	133.20	7.51E-03
	60	10.00	9.45	1984.50	198.45	5.04E-03
NSD	20	0.12	0.30	36.00	3.60	2.78E-01
	30	0.27	0.88	158.00	15.80	6.31E-02
	40	1.30	1.65	346.50	34.65	2.89E-02
	50	2.00	2.50	375.00	37.50	2.67E-02
	60	4.40	4.40	924.00	92.40	1.08E-02

3-4- The inhibition mechanism

In hydrochloric acid medium, the Fe surface is negatively charged due to the specifically adsorbed chloride ions on the surface. Owing to the acidity of the medium, the $-NH_2$ group in Dipron could not remain in solution as free base. It exists as a neutral species or in the cationic form as indicated below. Also, the oxygen and sulfure atoms in the sulfamidic group can be protonated easily, due to high electron density on it, leading to positively charged inhibitor species. Thus, Dipron inhibitor may adsorb through the electrostatic interactions between the positively charged Dipron molecules and the negatively charged Fe surface. Moreover, the adsorption of Dipron molecules could also be occurred due to the formation of links between the

d-orbital of Fe atoms, involving the displacement of water molecules from the metal surface, and the lonely sp^2 electron pairs present on the N and O atoms of the sulfamidic group [28].

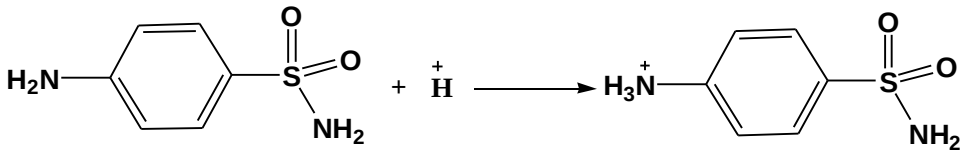

Molecular form Cationic form

Conclusions

1. From OCP, potentiodynamic and potentiostatic polarization measurements, the corrosion of Fe in HCl solutions is retarded in the presence of Dipron in MSD and NSD forms and the effect of NSD is more pronounced than MSD.
2. Dipron in MSD form could act as pickling inhibitor, while in NSD form could act as pickling inhibitor at high concentrations and behaves as mixed type but predominantly anodic inhibitor at low concentrations.
3. The inhibition efficiency increases with increasing Dipron concentration but decrease with increasing acid concentration and solution temperature.
4. 10 mM is considered as optimum concentration of Dipron for corrosion inhibition of Fe in 0.5M HCl solution.
5. The inhibition effect and corrosion protection increased as the particle size of inhibitor decreased even in small percentage in heterogeneous system.

References

1- 'Corrosion inhibition study of stainless steel in acidic medium – An overview', P. Selvakumar, B.B. Karthik and C. Thangavelu, Res. *J. Chem. Sci.*, **3**,4, pp87-95, 2013.

2- 'Ketorol: New and effective corrosion inhibitor for mild steel in hydrochloric acid solution', M.A. Quraishi, Sudheer and E.E. Ebenso, *Int. J. Electrochem. Sci.*, **7**, pp9920-9932, 2012.

3- 'Corrosion inhibition and adsorption properties of methocarbamol on mild steel in acidic medium', E.E. Ebenso, N.O. Eddy and A.O. Odiongenyi, *Port. Electrochim. Acta,* **27**, 1, pp13-22, 2009.
4- 'Quantum chemical studies on the corrosion inhibition of some sulphonamides on mild steel in acidic medium', T. Arslan, F. Kandemirli, E.E. Ebenso, I. Love and H. Alemu, *Corros. Sci.*, **51**, pp35-47, 2009.
5- 'Electrosynthesis and characterization of CdSeHgTl thin films', R.K. Pathak, *RJCS*, **3**, 4, pp44-47, 2013.
6- 'Expired Farcolin drug as corrosion inhibitor for carbon steel in 1M HCl solution', E.M. Attia, *J. Basic. Appl. Chem.*, **5**,1, pp1-15, 2015.
7- 'Ranitidine drugs as non-toxic corrosion inhibitors for mild steel in hydrochloric acid medium', R.S. Abdel Hameed, *Port. Electrochim. Acta*, **29**, 4, pp273-285, 2011.
8- 'Atlas of electrochemical equilibria in aqueous solutions', M. Pourbaix, 2nd Ed., NACE, Houston, TX, USA, pp307, 1974.
9- 'The influence of inorganic chemical accelerators and corrosion inhibitors on the mineralogy of hydrated Portland cement systems', M. Balonis. *Ph.D Thesis*, Department of Chemistry, University of Aberdeen, United Kingdom, 2010.
10- 'Inhibition of Fe corrosion using two newly synthesized Schiff base complexes in ethanolic hydrochloric acid media', E.M. Attia and Z.A. EL- Shafiey, *Al-Azhar Bull. Sci.*, **20**, 2, pp23-42, 2009.
11- 'Toxic potential of materials at the nanolevel', A. Nel, T. Xia, L. Mädler and N. Li, *Science*, **311**, pp622-627, 2006.
12- 'The effect of triazole thione derivative on the corrosion of Fe in hydrochloric acid solutions', E.M. Attia and F.H. Abdel- Salam, *Al-Azhar Bull. Sci.*, **20**, 2, pp43-58, 2009.
13- 'Nanosilicate extraction from rice husk ash as green corrosion inhibitor', D.A. Awizar, N.K. Othman, A. Jalar, A. Daudv, I. Abdul Rahman and N.H. Al-hardan, *Int. J. Electrochem. Sci.*, **8**, pp1759 – 1769, 2013.

14- 'Inhibiting effects of Rabeprazole sulfide on the corrosion of mild steel in acidic chloride solution', M.K. Pavithra, T.V. Venkatesha and M.K. Punith Kumar, *Int. J. Electrochem.*, **2013**, pp1-9, 2013.
15- 'Isotherm, kinetic and thermodynamic studies for the sorption of mercury (II) onto activated carbon from rosmarinus officinalis leaves', M. Erhayem, F. Al-Tohami, R. Mohamed and K. Ahmida, *Am. J. of Analy. Chem.*, **6**, pp1-10, 2015.
16- 'Influence of surface characteristics on liquid-phase adsorption of phenol by activated carbons prepared from bituminous coal', H. Teng and C. Hsieh, *Ind. Eng. Chem. Res.*, **37**, pp3618-3624, 1998.
17- 'Electrochemical behavior and corrosion inhibition of zinc electrode in solutions of $(NH_4)_2SO_4$ containing Ce (IV) ions', W.A.M. Hussein, E.M. Attia, I.M. Ghayad and W.A.M. Ghanem, *Researcher*, **6**,1, pp1-11, 2014.
18- 'Synthesis, characterization of some azo dyes derived from sulfa drugs and the use of them as corrosion inhibitors in 0.5 M hydrochloric acid solution', A.S. Abdul-Nabi and E.Q. Jasim, *Journal of Basrah Researches ((Sciences))*, **39**, 3, pp82-106, 2013.
19- 'Experimental and theoretical investigations anti-corrosive properties of Menthone on mild steel corrosion in hydrochloric acid', A. Ansari, M. Znini, I. Hamdani, L. Majidi, A. Bouyanzer and B. Hammouti, *J. Mater. Environ. Sci.*, **5**, 1, pp81-94, 2014.
20- 'Anti-corrosion inhibition of mild steel in 1 M hydrochloric acid solution by using *Tiliacora accuminata* leaves extract', R. Karthik, P. Muthukrishnan, S.M Chen, B. Jeyaprabha and P. Prakash, *Int. J. Electrochem. Sci.*, **10**, pp3707-3725, 2015.
21- '*Pavetta indica bark* as corrosion inhibitor in mild steel corrosion in HCl and H_2SO_4 medium: Adsorption and thermodynamic study', V.N. Sheeja and S. Subhashini, *Chem. Sci. Trans.*, **3**, 1, pp129-140, 2014.
22- 'Antibacterial drugs as inhibitors for the corrosion of stainless steel type 304 in HCl solution', A.S. Fouda, H.A. Mostafa and H.M. El-Abbasy, *J. Appl. Electrochem.*, **40**, 1, pp163-173, 2010.

23- 'Role of some thiadiazole derivatives as inhibitors for the corrosion of C-steel in 1 M H_2SO_4', A.S. Fouda, F.E. Heakal and M.S. Radwan, *J. Appl. Electrochem.*, **39**, 3, pp391-402, 2009.
24- 'Development of novel acidizing inhibitors for carbon steel corrosion in 15% boiling hydrochloric acid', A.R.S. Priya, V.S. Muralidharam and A. Subramania, *Corrosion*, **64**, 6, pp541-552, 2008.
25- 'Corrosion inhibition of carbon steel in hydrochloric acid solution by *Senna-Italica* extract', A.M. Al-Bonayan, *IJRRAS*, **22**, 2, pp49-64, 2015.
26- 'Electrochemical behavior of titanium electrode in aqueous bromide solutions', E.M. Attia, *Al-Azhar Bull. Sci.*, **17**, 2, pp53-71, 2006.
27- 'Fabrication of zinc-nano TiO_2 composite films: Electrochemical corrosion studies', M.K.P. Kumar and T.V. Venkatesha, *J. Chem. Pharm. Res.*, 5, 5, pp253-261, 2013.
28- 'Corrosion inhibition of mild steel in acidic medium by some sulfa drugs compounds', M.M. El-Naggar, *Corros. Sci.*, **49**, pp2226-2236, 2007.